Marine Pollution Bulletin 220 (2025) 118445

Contents lists available at ScienceDirect

Marine Pollution Bulletin

journal homepage: www.elsevier.com/locate/marpolbul

Impact of coastal deoxygenation on antibiotic resistance gene profiles in size-fractionated bacterial communities

Shujing Liu, Quanrui Chen, Changjie Dong, Xuanyun Qiu, Wenhao Li, Kai Tang *

State Key Laboratory of Marine Environmental Science, Fujian Key Laboratory of Marine Carbon Sequestration, College of Ocean and Earth Sciences, Xiamen University, China

ARTICLE INFO

Keywords:
Antibiotic resistance genes
Deoxygenation
Coastal seawater
Metagenomics

ABSTRACT

Oxygen loss disrupts marine ecosystems, threatening biodiversity and causing mass mortality of marine life. Antibiotic resistance genes (ARGs) pose a significant threat to human health by promoting the spread of resistant pathogens, making infections harder to treat and increasing mortality risks. However, the interplay between deoxygenation and ARG dynamics remains poorly understood. In this study, we employed time-series metagenomics to investigate the responses of ARG profiles in free-living (FL) and particle-associated (PA) fraction to oxygen loss during a 22-day summer deoxygenation event in the East China Sea. In total, we identified 1,186 ARG subtypes and 2,279 mobile genetic element (MGE) subtypes. The most dominant resistance classes of antibiotics were multidrug (23.5%), followed by tetracycline (15%), macrolide-lincosamide-streptogramin (13.4%), peptide (10.3%), glycopeptide (8.7%), aminoglycoside (7.3%), and beta-lactam (4.9%). We found that ARG richness in FL fraction increased with declining oxygen levels, particularly for beta-lactam and multidrug class, while no significant relationship was observed in the PA fraction. Although the total relative abundance of ARGs in both fraction showed no significant oxygen dependence, beta-lactam and multidrug resistance genes in FL fraction significantly increased with oxygen loss. Co-occurrence network analysis revealed stronger positive associations between ARGs and MGEs in the FL fraction, suggesting enhanced gene transfer among environmental bacteria. Furthermore, neutral community model analysis indicated that stochastic processes also played an interactive role in shaping ARG composition dynamics in both bacterial fractions. Our findings provide evidence that coastal deoxygenation preferentially enriches high-risk ARGs (e.g., beta-lactamase genes) in FL bacteria through MGE-mediated transfer, highlighting escalating antibiotic resistance risks that threaten both ecosystem and human health under climate warming. This study offers a framework for size-fractionated ARG monitoring and targeted mitigation strategies in coastal ecosystems.

1. Introduction

Antimicrobial resistance poses a growing global threat to human health and clinical disease treatment (Allen et al., 2010). Antibiotic resistance genes (ARGs), recognized as emerging contaminants, are pervasive in marine environments, serving as critical reservoirs for antibiotic-resistant bacteria and ARGs worldwide (Xu et al., 2023). In aquatic ecosystems, ARGs threaten biodiversity, ecosystem functions, and public health by contributing to hard-to-treat infections transmitted through contaminated water, recreational activities, and food consumption (Zheng et al., 2021; Lyautey et al., 2021). The impact of antibiotics and ARGs on microbial communities has been widely evidenced in global estuarine and coastal environments, with studies showing a decrease in microbial community richness and diversity following antibiotic exposure in estuarine sediments (Harrabi et al., 2019). Anthropogenic activities, particularly clinical antibiotic overuse, terrestrial runoff, and intensive aquaculture, are primary drivers of ARG dissemination (Zhang et al., 2022). As the largest global producer and consumer of antibiotics, China faces heightened risks of ARG pollution in its coastal waters (Zhang et al., 2015). With one of the world's longest coastlines, China's coastal ecosystems are pivotal reservoirs and transmission pathways for ARG proliferation. Coastal zones, positioned at the interface of terrestrial and marine systems, exhibit particularly high ARG abundance and diversity, underscoring the urgency to study their dynamics in these ecologically and economically vital regions (Zhu et al., 2017).

* Corresponding author.
E-mail address: tangkai@xmu.edu.cn (K. Tang).

https://doi.org/10.1016/j.marpolbul.2025.118445
Received 26 March 2025; Received in revised form 27 May 2025; Accepted 10 July 2025
Available online 15 July 2025
0025-326X/© 2025 Elsevier Ltd. All rights are reserved, including those for text and data mining, AI training, and similar technologies.

Deoxygenation is a major threat to oceans, driving mass mortality of fish and benthic invertebrates (Vaquer-Sunyer and Duarte, 2008; Breitburg et al., 2018) and altering bacterial community structure (Beman and Carolan, 2013). Global warming, which reduces oxygen solubility in water, and nutrient loading from human activities, which increases oxygen consumption through respiration, have exacerbated deoxygenation events (Breitburg et al., 2018; Keeling et al., 2010; Chen and Guo, 2020). Since the mid-20th century, oxygen concentrations in both open ocean and coastal waters have been steadily declining (Stramma et al., 2008). Certain areas of the ocean experience critically low or even absent oxygen levels, with the most severe conditions found in the subsurface waters of the Arabian Sea and the eastern tropical upwelling regions off the coasts of California, Peru, and Namibia (Karstensen et al., 2008). As significant reservoirs of ARGs, bacterial assemblages are closely linked to ARG profiles (Larsson and Flach, 2022). While numerous studies have documented ARGs in marine systems (Wen et al., 2025; Wen et al., 2024; Li et al., 2023), the impact of marine deoxygenation on ARG distribution remains poorly understood. Furthermore, bacterial communities are typically categorized as free-living or particle-associated bacteria based on their lifestyle (Grossart, 2010), but the differential responses of their ARGs to environmental stressors remain underexplored. Addressing these knowledge gaps is critical for predicting ARG dissemination risks in rapidly changing marine ecosystems.

Intensifying eutrophication, driven by anthropogenic nutrient inputs, has led to seasonal oxygen loss in coastal waters around China, such as the Bohai Sea and the East China Sea (Chen et al., 2007; Luo et al., 2009; Guo et al., 2020). Notably, a record-breaking global heatwave of 2022 amplified these conditions, contributing to a significant deoxygenation event in the East China Sea (Tan et al., 2023; Shinohara et al., 2023). The resulting oxygen gradients in the East China Sea provide a unique natural laboratory to investigate the effects of oxygen gradient on ARG profiles. Capitalizing on this natural experiment, we collected 93 metagenomic samples to investigate ARG profiles in both free-living (FL) and particle-associated (PA) bacterioplankton over a 22-day period in the coastal waters. The objectives of this study were to: (1) determine the spatiotemporal variation of ARGs in FL and PA fractions within the East China Sea; (2) assess the response of ARG functional diversity and distribution to oxygen loss; and (3) elucidate the roles of selective and neutral processes in driving antibiotic resistant community assembly in FL and PA fractions. This study improves our understanding of comprehensive ARG profiles in coastal systems.

2. Materials and methods

2.1. Sample collection

Water samples were collected from two sites near Zhoushan in the East China Sea during July to August 2022 (Fig. 1). At each site, samples were collected from three distinct water layers: surface (A1: 3 m; C4: 5 m), middle (A1: 17 m; C4: 25 m), and bottom (A1: 40 m; C4: 60 m). Environmental parameters, including dissolved oxygen concentration, pH, temperature, and salinity, were measured in situ using OCEAN SEVEN 316Plus CTD sensor (Idronaut, Italy). Additionally, dissolved oxygen measurements were further validated through calibration using a dissolved oxygen bottle equipped with an optical oxygen sensor (PreSens, Germany), with readings taken from the surface, middle, and bottom layers, and analyzed using a fiber-optic oxygen meter (PreSens, Germany). Prior to the fieldwork, all probes underwent stringent calibration to ensure accuracy, and during sampling, we ensured the consistency of dissolved oxygen data by comparing the sensor readings with atmospheric oxygen levels. For each sample, 10 L of water was first pre-filtered through a 20 μm nylon mesh to remove larger particles. It was then sequentially filtered through 3 μm and 0.2 μm membrane filters to separate microbial communities into two fractions: particle-associated microorganisms (retained on the 3 μm filter) and free-living microorganisms (retained on the 0.2 μm filter). To minimize potential contamination, all filtration equipment was treated with acid baths prior to use.

2.2. Metagenomics sequencing and annotation

The 0.2 μm and 3 μm filter membranes were cut into strips and subjected to ultrasonic oscillation to detach bacterial cells. The resulting mixture was centrifuged to concentrate the suspensions, and total

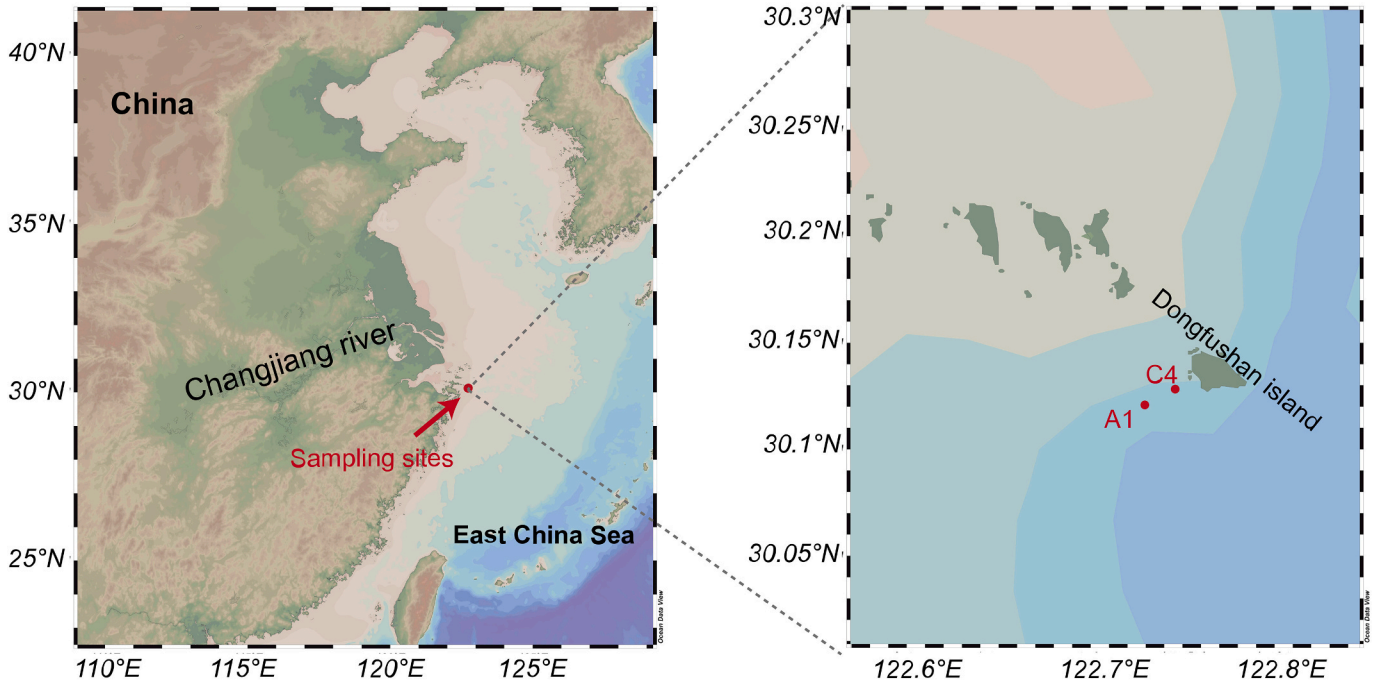


Fig. 1. Map showing the sampling stations in the East China sea. Red dots indicate the locations where seawater samples were collected. (For interpretation of the references to colour in this figure legend, the reader is referred to the web version of this article.)

genomic DNA was extracted using the DNeasy PowerSoil Kit (MoBio, USA) according to the manufacturer's instructions. The DNA extraction process was carried out following strict standardized protocols. Additionally, the 16S rRNA gene sequencing results revealed a microbial community composition dominated by SAR11 and Rhodobacterales (Liu et al., 2024), which is consistent with typical microbial profiles observed in estuarine studies, indicating that the samples were not contaminated. The extracted DNA was sequenced on the NovaSeq 6000 platform with Illumina PE150 chemistries at Hanyu Bio-Tech (Shanghai, China), yielding at least 10 Gb of total bases per sample.

2.3. Annotation of ARGs and mobile genetic elements (MGEs)

After quality control by Trimmomatic v0.36 (Bolger et al., 2014), the clean reads were assembled using Megahit v1.1.3 (Li et al., 2016). Open reading frames (ORFs) in contigs were predicted using Prodigal v2.6.3 (−p meta) (Hyatt et al., 2010). The non-redundant ORFs catalog was constructed using CD-HIT v4.8.1 (−c 0.95, -aS 0.9) (Fu et al., 2012). Gene abundance was quantified using Samtools v1.7 by transcripts per million (TPM) (Li et al., 2009). To identify ARGs and MGEs, protein sequences from the non-redundant ORFs catalog were aligned against the CARD database (Jia et al., 2017) and ISfinder database (Siguier et al., 2006) using DIAMOND v2.0.7 (Buchfink et al., 2015). ARGs were manually reclassified based on the antibiotic classes they confer resistance to, following established methodologies from prior literature (Zhang et al., 2022). Specifically, ARGs targeting penams, cephalosporins, carbapenems, cephamycins, penems, and monobactams were categorized into the beta-lactam class. Genes associated with resistance to macrolides, lincosamides, and streptogramins were grouped into the macrolide-lincosamide-streptogramin (MLS) class. ARGs conferring resistance to multiple distinct drug classes were classified under the multidrug class.

2.4. Statistical analysis

To explore the effect of oxygen loss on ARGs diversity, we performed linear regressions and Pearson's correlation coefficient on the Bray-Curtis dissimilarity of ARG richness versus oxygen concentration. Network analysis was performed to investigate the co-occurrence patterns of ARGs and MGEs. Spearman's rank correlations with $r > 0.7$ and $p < 0.01$ were selected for further illustration in networks. Gephi v0.10.1 was used for the visualization of networks (Bastian et al., 2009). According to previous research (Guo et al., 2018), we used a neutral community model (NCM) to evaluate the importance of stochastic processes in ARG community assembly between FL and PA fractions (Sloan et al., 2006; Chen et al., 2019). All analyses and graphical visualizations were performed in R (Team RC, 2022).

3. Results

3.1. Environmental parameters during the sampling period

Throughout the sampling period, there were significant vertical differences in the environmental factors (dissolved oxygen, pH, salinity, and temperature) at the A1 and C4 stations (Fig. S1). Fluctuations in these parameters were particularly notable at the surface layer throughout the observation period. At the A1 station, dissolved oxygen levels ranged from 2.73 to 10.01 mg/L (Fig. S1a), while at the C4 station, they varied from 3.11 to 9.58 mg/L (Fig. S1b). Although the dissolved oxygen levels did not reach hypoxic conditions, the bottom layers at both stations consistently showed significantly lower oxygen concentrations compared to the surface ($p < 0.05$), with these waters experiencing substantial deoxygenation events. These differences highlight the pronounced vertical stratification of oxygen levels, as well as the dynamic changes in surface parameters during the study period.

3.2. Overview of total ARGs of FL and PA fraction in the East China Sea

Overall, metagenomics analysis identified 136,256 sequences annotated as ARGs, belonging to 1,186 antibiotic resistance subtypes spanning 23 major resistance classes (Fig. 2a and b). These ARGs encompassed six resistance mechanisms including antibiotic efflux (60.9%), antibiotic target alteration (21.1%), antibiotic target protection (6.4%), antibiotic inactivation (4.5%), antibiotic target replacement (4.4%), and reduced permeability to antibiotic (2.7%) (Fig. S2a). The detected ARGs potentially conferred resistance to almost all major classes of antibiotics, with multidrug (23.5%), tetracycline (15%), MLS (13.4%), peptide (10.3%), glycopeptide (8.7%), aminoglycoside (7.3%), and beta-lactam (4.9%) contributing the most of detected ARG relative abundance (Fig. S2b). The richness and relative abundance of ARGs in FL fraction were higher than that in PA fraction ($p < 0.05$). Additionally, we identified 38,860 sequences as MGEs, belonging to 2,279 MGEs subtypes, contributing to 2.4% of all identified ARGs (Fig. 2c and d).

3.3. Effects of oxygen decline on ARG profiles between FL and PA fraction

Oxygen concentration exhibited differential impacts on the richness of antibiotic resistant communities between FL and PA fractions. A significant negative correlation was observed between dissolved oxygen levels and FL ARG richness (Pearson's $r = -0.51$, $p < 0.001$), whereas PA ARG richness showed no oxygen-dependent pattern (Pearson's $r = -0.19$, $p > 0.05$) (Fig. 3a). Notably, the overall relative abundance of ARGs in both fractions showed oxygen-independent characteristics ($p > 0.05$) (Fig. 3b). Detailed analysis of FL ARG classes revealed oxygen-mediated regulation of diversity patterns (Fig. 4). The richness of major FL ARG classes, including multidrug, tetracycline, MLS, peptide, glycopeptide, aminoglycoside, and beta-lactam increased with oxygen decline (Fig. 4a), particularly beta-lactam (Pearson's $r = -0.50$, $p < 0.001$), followed by multidrug (Pearson's $r = -0.47$, $p < 0.001$). While the total relative abundance of ARGs in both FL and PA fractions showed no significant relationship with oxygen levels, the relative abundance of specific ARG classes, including multidrug (Pearson's $r = -0.31$, $p < 0.05$) and beta-lactam (Pearson's $r = -0.33$, $p < 0.05$) significantly increased with oxygen loss (Fig. 4b). Principal coordinates analysis based on Bray-Curtis distances further revealed subtle but statistically significant differences in ARG composition across oxygen concentrations (Fig. 5). Additionally, other environmental factors, such as temperature, pH, and salinity, were significantly correlated with FL richness but showed no significant relationship with the PA fraction (Fig. S3).

3.4. Response of MGEs to environmental variables between FL and PA fraction

Given the close relationship between ARGs and MGEs, we further investigated the influence of oxygen levels on MGE dynamics. Our results revealed distinct patterns between FL and PA communities (Fig. 6). For FL communities, both MGEs richness and relative abundance exhibited significant negative correlations with oxygen concentration (richness: Pearson's $r = -0.48$, $p < 0.001$; abundance: Pearson's $r = -0.37$, $p < 0.001$). In contrast, PA communities showed no significant relationship between oxygen levels and either MGEs richness (Pearson's $r = -0.22$, $p > 0.05$) or abundance (Pearson's $r = -0.10$, $p > 0.05$).

3.5. Assembly processes of ARGs and MGEs

The community assembly processes of ARG and MGE profiles were explored using the NCM. The NCM explained a moderate fraction of the variation in ARG composition in all bacteria ($R^2 = 0.58$) in the 93 samples (Fig. 7). When analyzed separately, ARGs in both free-living and particle-associated bacteria exhibited a good fit to the NCM, with R^2 values of 0.61 and 0.58, respectively (Fig. 7a). Similarly, the NCM

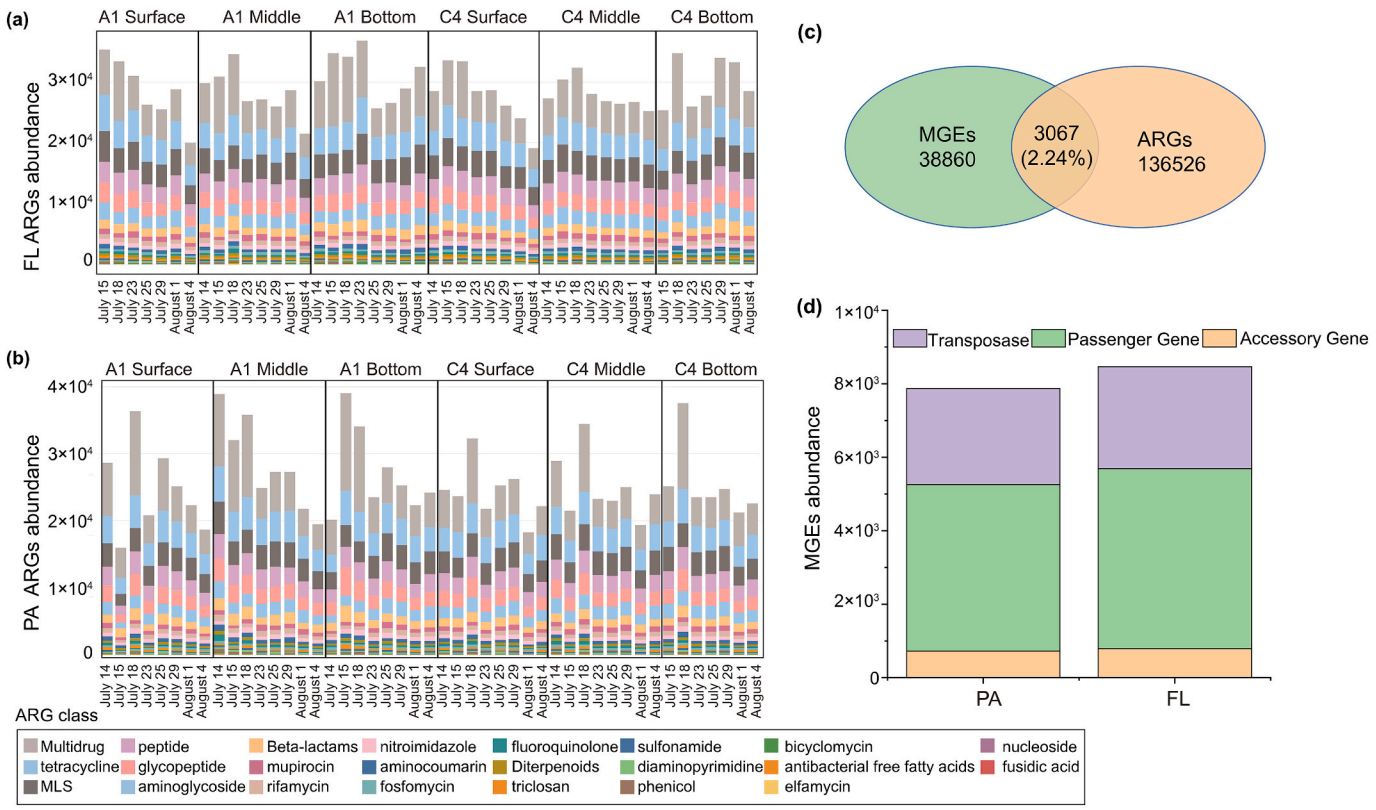


Fig. 2. Distribution of ARGs in the free-living fraction (a) and particle-associated fraction (b). Venn diagrams illustrate the overlap and unique sequences of MGEs and ARGs identified in metagenomic data (c). The relative abundance of MGEs is shown in (d).

explained a moderate fraction of the variation in MGE composition across all bacterial samples ($R^2 = 0.48$). The MGEs in FL and PA bacteria also displayed a reasonable fit to the NCM, with R^2 values of 0.50 and 0.47, respectively (Fig. 7b).

3.6. Co-occurrence network between the ARGs and MGEs

Spearman's correlation was used to compute the relationships between ARGs and MGEs in both FL and PA fractions (Fig. 8). In the FL fraction, the co-occurrence network comprised 1,788 nodes (671 ARGs and 1,117 MGEs) connected by 10,111 edges (Fig. 8a). The PA network contained 1,601 nodes (665 ARGs and 936 MGEs) with 9,322 edges (Fig. 8b). We further found that MGEs were significantly and positively correlated with genes conferring resistance to beta-lactam, multidrug, MLS, and aminoglycoside ($p < 0.01$). Topological analysis showed that key parameters, including average degree, average weighted degree, average path length, network diameter, and graph density, were slightly higher in the PA fraction compared to the FL fraction. In both FL and PA fractions, beta-lactam resistance genes accounted for 34% of all ARG nodes, dominating the ARG composition, followed by multidrug resistance genes (16%).

4. Discussion

4.1. Oxygen decline increased the richness of free-living ARGs

Our study provides in situ evidence that oxygen decline significantly increases the diversity of ARGs in FL bacterial communities, particularly for beta-lactam and multidrug resistance genes (Figs. 3 and 4). This pattern may be attributed to two synergistic mechanisms driven by human activities and microbial evolutionary responses. Firstly, the high anthropogenic input in coastal ecosystems creates a dual selection pressure. Pharmaceutical pollution, particularly in the form of antibiotic residues (such as beta-lactams and multidrug combinations), serves as a persistent selective force, while oxygen depletion induces metabolic stress on bacterial communities (Beman and Carolan, 2013). In estuarine areas like the Changjiang river, substantial quantities of beta-lactam antibiotics are discharged from adjacent megacities into the East China Sea (Yan et al., 2013), and multidrug resistance residues are frequently detected due to overuse in clinical settings (Yezli and Li, 2012). Beta-lactams are among the most extensively used classes of antibiotics for human and veterinary use (Carvalho and Santos, 2016), and multidrug resistance genes confer resistance to multiple distinct drug classes. Under normoxic conditions, most antibiotics degrade rapidly, but oxygen level declining significantly reduces the degradation rate due to the limited availability of aerobic degradation pathways (Jong et al., 2020). In addition, human activities such as aquaculture and wastewater discharge further exacerbate the problem, introducing additional contaminants and nutrients that can alter microbial community structure and function (Wakelin Steven et al., 2008). Consequently, antibiotic residues persist longer in deoxygenated environments, amplifying the selection pressure for corresponding ARGs.

Secondly, oxygen depletion fundamentally alters microbial survival strategies. Deoxygenation induces oxidative stress and limits energy production through aerobic respiration (Breitburg et al., 2018), compelling bacteria to prioritize energy-efficient mechanisms for antibiotic resistance. Bacteria that already harbor pre-adapted ARGs, especially those located on MGEs such as plasmids, gain a competitive advantage. We observed that oxygen decline increased the diversity of MGEs in all communities (Fig. 6). Variation in mobile genetic elements contributes to the diversification of bacterial populations, gene regulation, and the potential for the spread of resistance traits, increasing the overall risk of disease transmission (Kojima et al., 2023). Our network analysis reveals that beta-lactam and multidrug resistance ARGs exhibit stronger connectivity with MGEs compared to other ARG classes (Fig. 8),

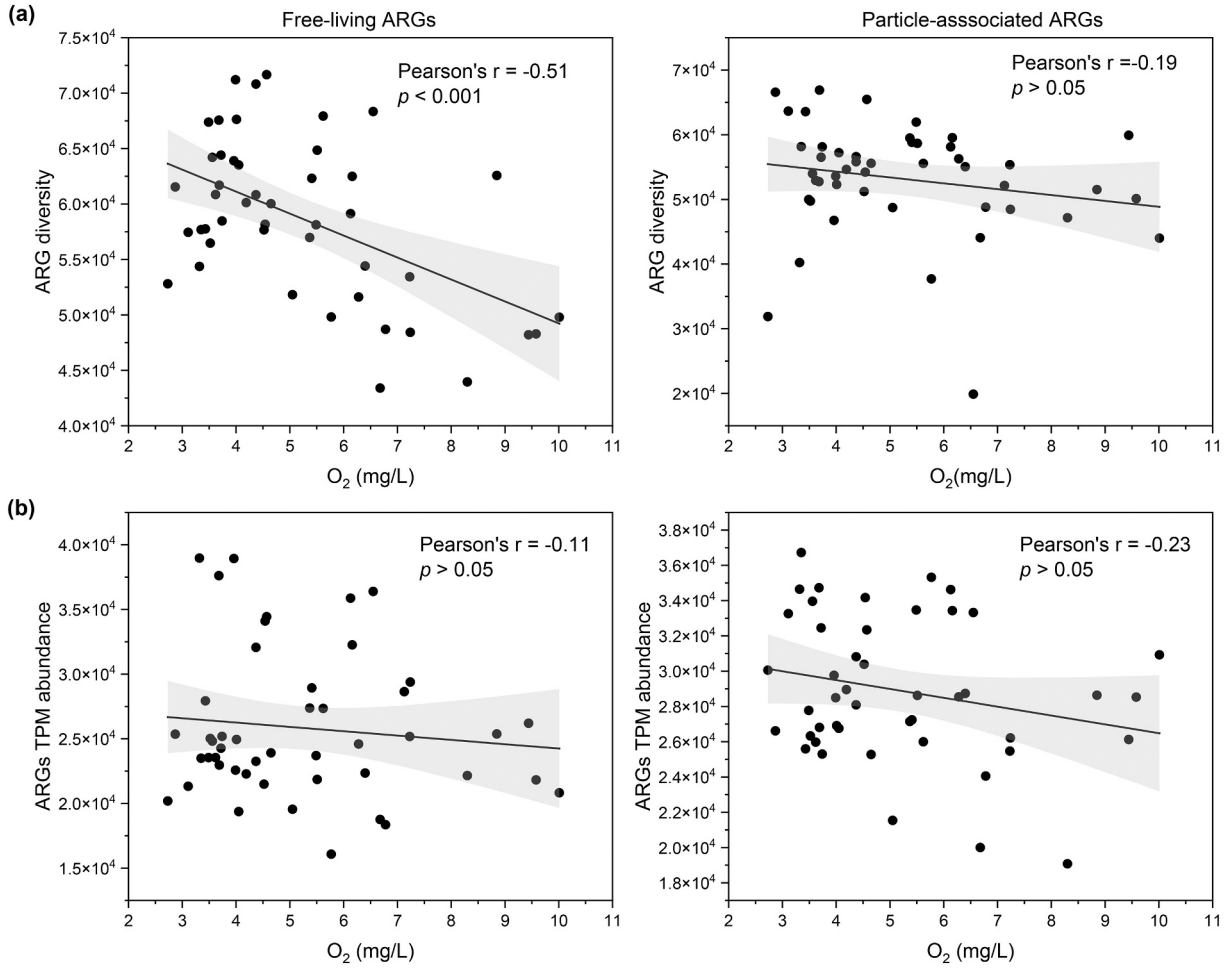


Fig. 3. Linear regression between ARGs richness (a) and relative abundance (b) against oxygen level.

suggesting these genes are preferentially maintained on transferable elements under environmental stress. This is consistent with studies suggesting that hypoxia can indirectly enhance plasmid conjugation efficiency by inducing oxidative stress and upregulating integrase gene expression (Huang et al., 2022).

The combination of human-made antibiotic residues and low-oxygen conditions in coastal waters creates a challenging environment for marine ecosystems. Beta-lactamase genes not only confer resistance to penicillins and cephalosporins, but may also enhance bacterial survival through collateral benefits. For example, some metallo-beta-lactamases exhibit catalase-like activity, helping bacteria mitigate oxidative stress (Liu et al., 2021). These may explain why beta-lactam and multidrug resistance ARGs increased in deoxygenated zones, despite fluctuating antibiotic concentrations. Furthermore, the expansion of marine low-oxygen areas due to climate change accelerates the accumulation of high-risk ARGs in coastal environments, posing a serious threat to human health.

4.2. Different effects of oxygen decline on abundance and composition of ARGs between FL and PA fraction

Our results demonstrated different responses of ARG profiles between FL and PA fractions to oxygen decline (Fig. 3). Quantitative evidence indicates that deoxygenation exerts a more pronounced promotional effect on ARG diversity and class-specific relative abundance in the FL fraction compared to the PA fraction (Figs. 3 and 4). This is consistent with a previous report that FL bacterial communities are more sensitive to oxygen deficiency than PA bacterial communities in the Bohai Sea (Zhao et al., 2021). Our earlier finding also revealed that PA communities exhibit greater stability in the face of organic matter disturbance (Liu et al., 2024). In freshwater reservoirs, cyanobacterial blooms appear to have a stronger inhibitory effect on ARG abundance in FL bacteria, and a stronger influence on antibiotic-resistant community composition in PA bacteria (Guo et al., 2018). While our PCoA confirmed that oxygen levels have a significant but slight effect on ARG composition (Fig. 5), this divergence may be due to the higher environmental connectivity in marine systems compared to freshwater reservoirs.

The relative stability of PA bacteria may arise from several interrelated mechanisms. Firstly, particulate matter provides a stable microenvironment that buffers PA bacteria from environmental stressors, including oxygen fluctuations, helping them maintain metabolic activity despite deoxygenation (Dang and Lovell, 2016). This physical protection reduces the impact of oxygen depletion on PA bacteria. Secondly, PA bacteria often form biofilms on particulate matter, enhancing their stability. Biofilms act as a barrier, protecting bacteria from oxidative stress and nutrient limitation, while also reducing the horizontal transfer of ARGs due to less efficient gene exchange in biofilm environments (Meinhard et al., 2002). Additionally, particulate matter serves as a localized nutrient reservoir, improving resource acquisition and metabolic efficiency, which helps PA bacteria withstand oxygen changes by reducing reliance on surrounding water chemistry (Dang and Lovell, 2016).

In contrast, the free-living fraction is more directly exposed to oxygen disturbance, and the lifestyle preference of FL bacteria could potentially facilitate the exchange of genetic material encoding

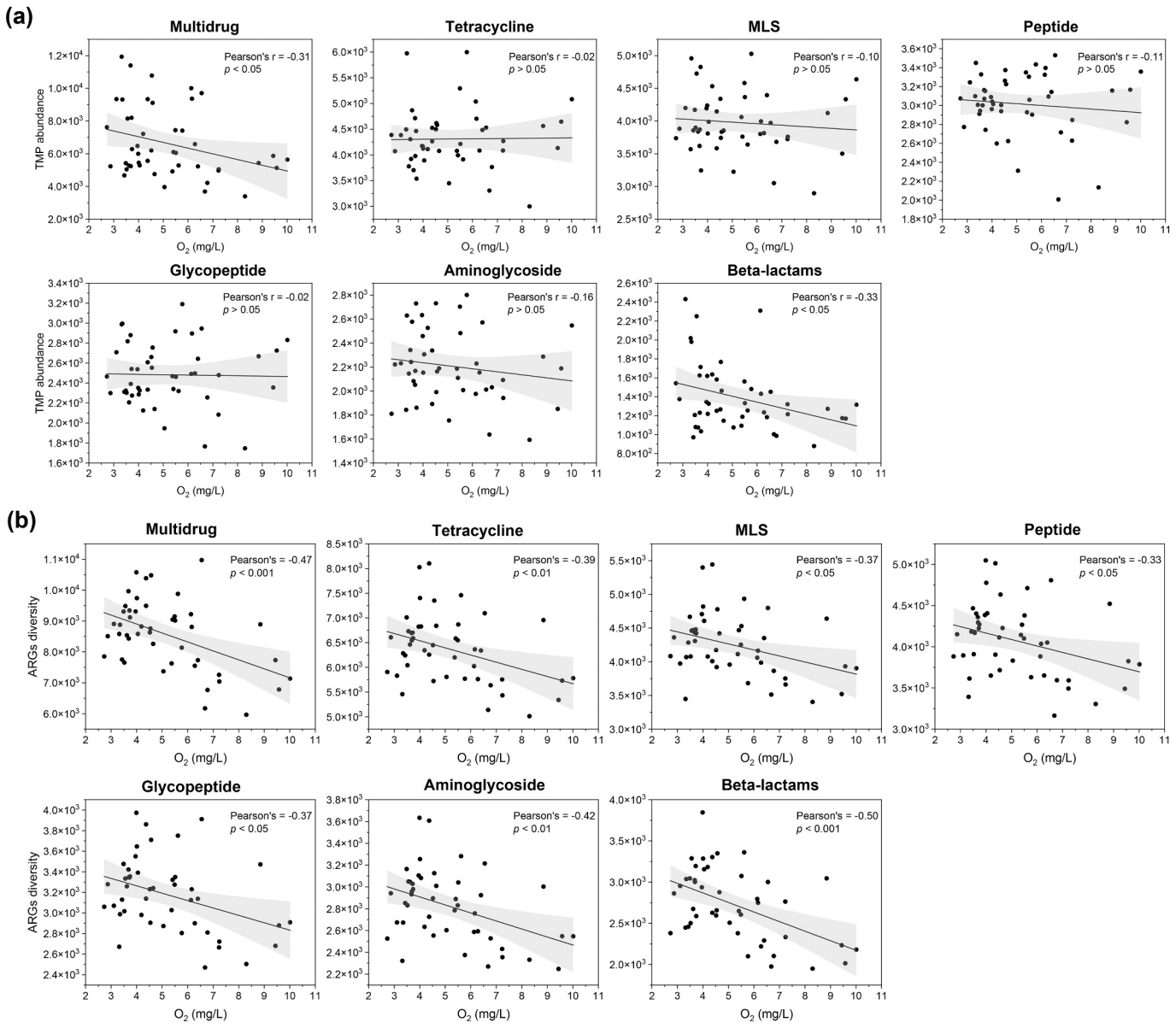


Fig. 4. Linear regression of major ARG type richness (a) and relative abundance (b) against oxygen level in the free-living fraction.

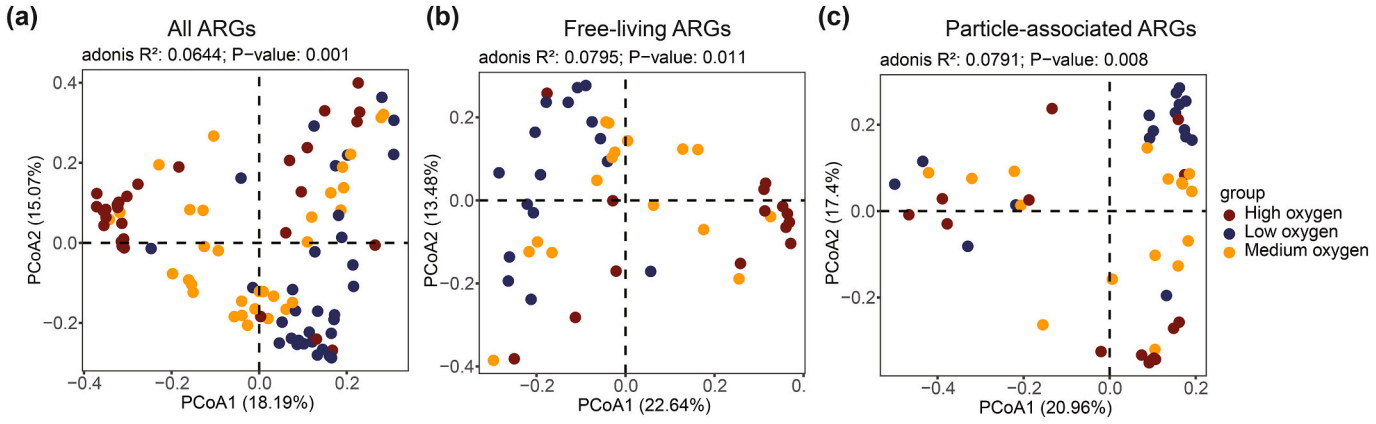


Fig. 5. Principal Coordinates Analysis (PCoA) of ARGs based on Bray-Curtis dissimilarity: (a) all ARGs, (b) free-living ARGs, and (c) particle-associated ARGs. Samples are grouped by oxygen levels: high oxygen (6–10 mg/L), medium oxygen (4–6 mg/L), and low oxygen (0–4 mg/L) and indicated by distinct colors.

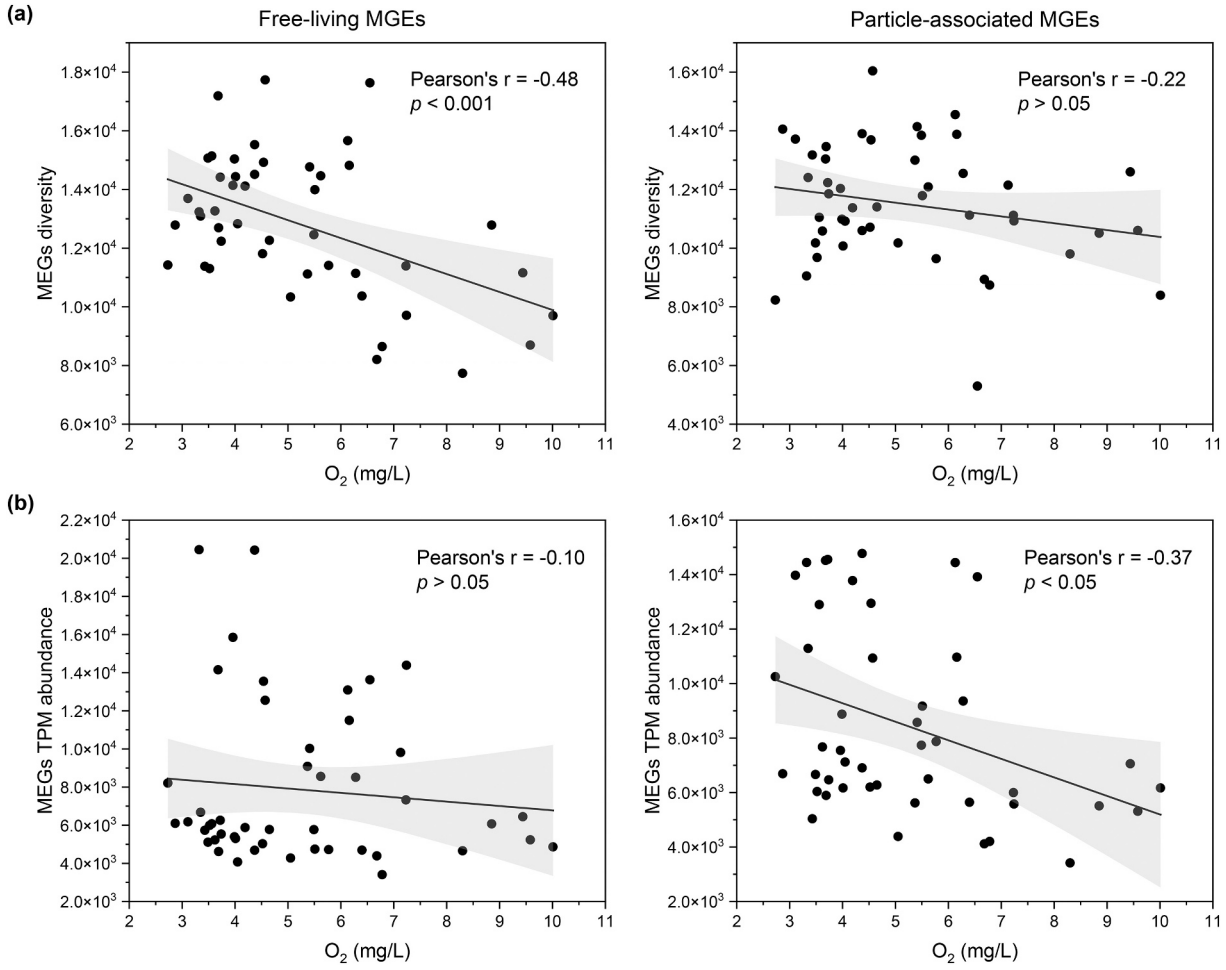


Fig. 6. Linear regression between MGEs richness (a) and relative abundance (b) against oxygen level.

resistance (Guo et al., 2018). In this study, stronger positive correlations between ARGs and MGEs were found in the FL fraction compared to the PA fraction, which may facilitate horizontal gene transfer of ARGs via MGEs (Fig. 8). This differential interaction may partially explain the heightened sensitivity of ARGs in FL fraction to oxygen fluctuations, as their planktonic lifestyle likely increases exposure to physicochemical shifts that promote MGE-mediated genetic exchange. Additionally, major effects induced by deoxygenation may lead to alterations in the function of expressed genes or proteins to better suit the changed environment (Hawley et al., 2014), and the free-living fraction may enhance the abundance, motility, and pathogenic potential of the resistome to adapt to environmental disturbance (Xu et al., 2023).

4.3. The importance of stochastic process in the assembly of ARGs

Our NCM analysis revealed significant stochastic influences on ARG profiles ($R^2 = 0.58$), suggesting that neutral processes dominate ARG assembly in the East China Sea (Fig. 7). The NCM is widely applied to quantify stochasticity in bacterial taxonomic assembly, but has not been extensively used to quantify the role of neutral process in ARGs assembly (Guo et al., 2018; Chen et al., 2019). ARGs in FL bacteria exhibited a higher level of stochastic processes than those in PA bacteria (FL: $R^2 = 0.61$, PA: $R^2 = 0.58$) (Fig. 7). Similarly, MGE assembly demonstrated lower overall stochasticity compared to ARGs ($R^2 = 0.48$), yet MGEs in FL bacteria still displayed a higher stochastic influence than those in PA bacteria. This pattern may be attributed to the limited dispersal capacity of PA bacteria due to their attachment to particles. In contrast, ARGs and MGEs in the FL fraction experience fewer dispersal barriers, allowing stochastic colonization to play a larger role. The importance of stochastic processes in ARGs assembly within our studied areas diverges sharply from findings in freshwater lakes, where deterministic processes dominate the assembly of ARGs ($R^2 = 0.10$) (Hou et al., 2025). This discrepancy is likely driven by intense coastal currents in marine system, enhancing microbial dispersal and homogenization (Chen et al., 2019). These findings establish hydrological connectivity as a crucial factor modulating ARG dissemination pathways. Understanding the role of stochasticity in ARG assembly is essential for predicting the spread of antibiotic resistance, particularly in the context of climate-driven ocean deoxygenation.

5. Conclusion

In this study, the distribution patterns of ARG profiles in FL and PA bacterial communities under deoxygenation in the East China Sea were analyzed via metagenomics. Our findings demonstrated that ARG richness in FL fraction significantly increased with declining oxygen levels, particularly for high-risk beta-lactam and multidrug resistance genes, whereas no such trend was observed in the PA fraction. Although the total relative abundance of ARGs in both fractions showed no significant dependence on oxygen levels, the abundance of beta-lactam and multidrug resistance genes in FL fraction significantly increased with oxygen loss. Strong correlations between ARGs and MGEs indicated that MGEs were important mechanisms of ARG dynamics and dissemination under changing environments. Additionally, neutral community model analysis highlighted the interactive role of stochastic processes in shaping ARG composition, emphasizing the influence of hydrodynamic

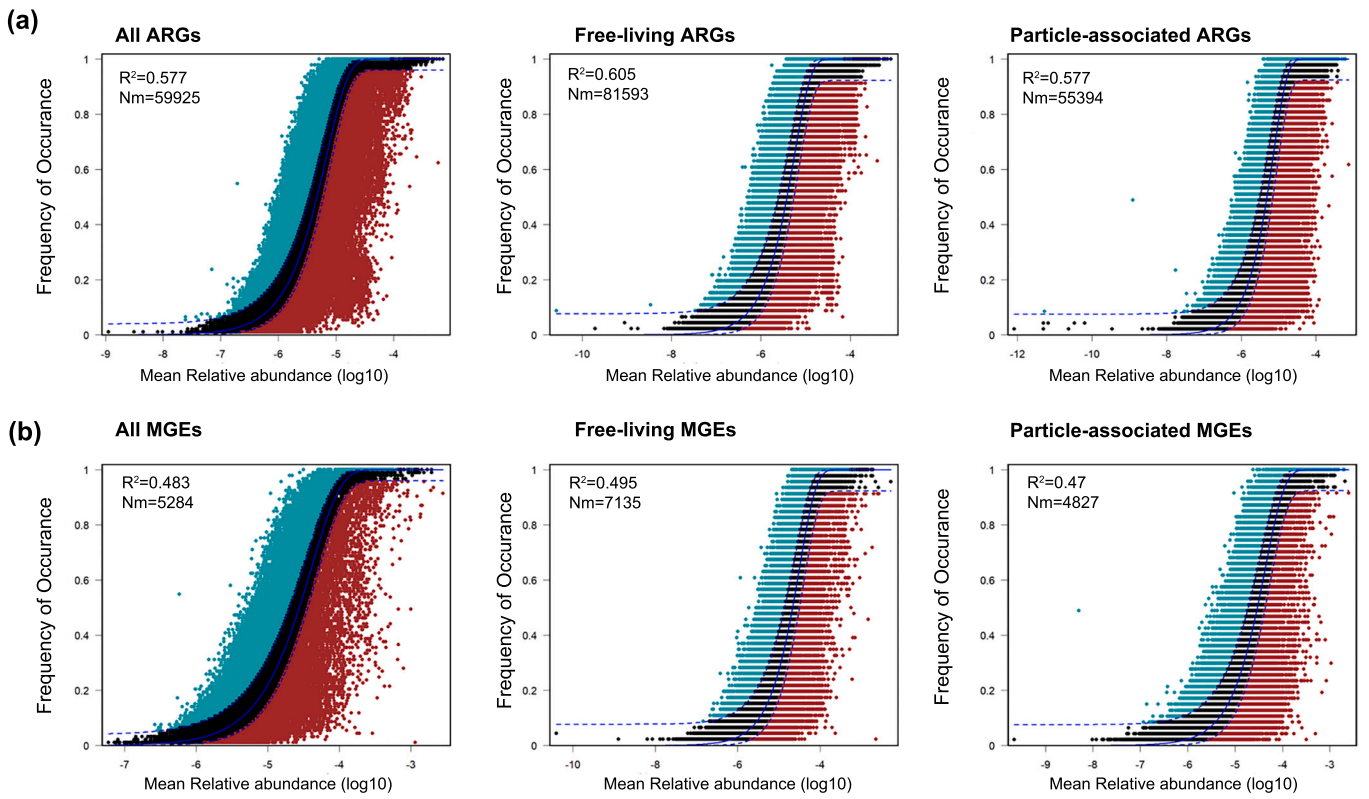


Fig. 7. NCM fit for community assembly, showing predicted occurrence frequencies of ARGs (a) and MGEs (b). R^2denotes the model fit.

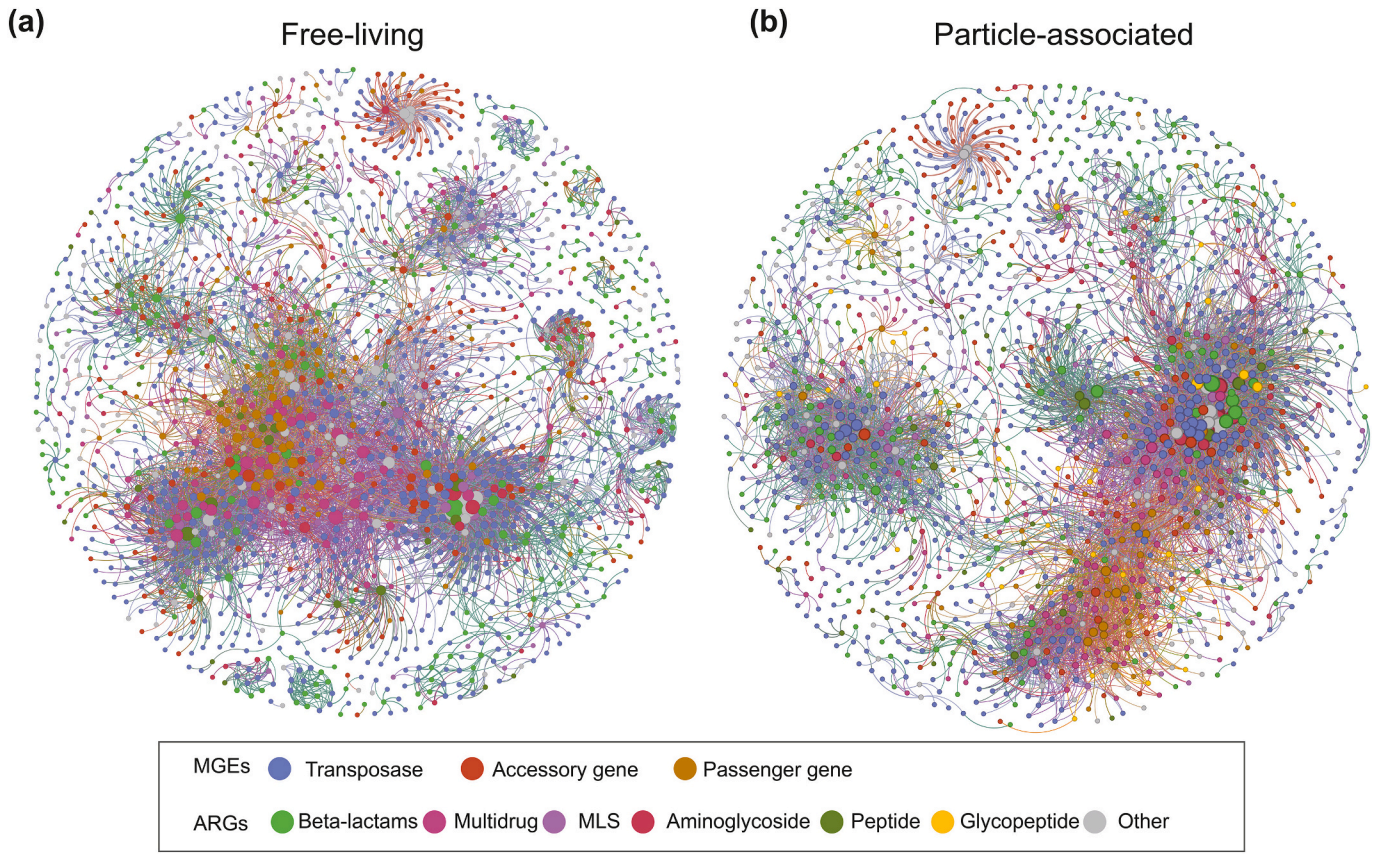


Fig. 8. Co-occurrence network of ARGs and MGEs in free-living (a) and particle-associated fractions (b). Node colors represent ARGs and MGEs classes, and node size indicates average degree (number of connections).

connectivity on ARG dissemination. Given the increasing frequency and severity of coastal deoxygenation under climate change, our results underscore the urgent need for targeted monitoring and mitigation strategies to curb the spread of antibiotic resistance. Specifically, implementing real-time monitoring of ARGs and MGEs in coastal areas, alongside the development of targeted mitigation strategies such as reducing nutrient loading and controlling pollution, could help prevent the exacerbation of ARG contamination. Additionally, improving public awareness and policies regarding coastal ecosystem health could play a key role in managing the risks of antibiotic resistance in these vulnerable environments.

CRediT authorship contribution statement

Shujing Liu: Writing – review & editing, Writing – original draft, Visualization, Methodology, Investigation, Formal analysis, Data curation. **Quanrui Chen:** Writing – review & editing, Methodology, Investigation. **Changjie Dong:** Writing – review & editing, Methodology, Investigation. **Xuanyun Qiu:** Writing – review & editing, Methodology, Investigation. **Wenhao Li:** Writing – review & editing, Methodology, Investigation. **Kai Tang:** Writing – review & editing, Writing – original draft, Supervision, Resources, Project administration, Funding acquisition.

Declaration of competing interest

The authors declare that they have no known competing financial interests or personal relationships that could have appeared to influence the work reported in this paper.

Acknowledgments

This study was supported by the National Natural Science Foundation of China project (42141003, 92251306), and the Ocean Negative Carbon Emissions (ONCE).

Appendix A. Supplementary data

Supplementary data to this article can be found online at https://doi.org/10.1016/j.marpolbul.2025.118445.

Data availability

The sequences of metagenome raw data have been uploaded to the National Omics Data Encyclopedia (NODE, https://www.biosino.org/node/) database with the identifier OEX00024201.

References

Allen, H.K., Donato, J., Wang, H.H., Cloud-Hansen, K.A., Davies, J., Handelsman, J., 2010. Call of the wild: antibiotic resistance genes in natural environments. Nat. Rev. Microbiol. 8 (4), 251–259.
Bastian, M., Heymann, S., Jacomy, M., 2009. Gephi: an open source software for exploring and manipulating networks. Proceedings of the International AAAI Conference on Web and Social Media 3 (1), 361–362.
Beman, J.M., Carolan, M.T., 2013. Deoxygenation alters bacterial diversity and community composition in the ocean's largest oxygen minimum zone. Nat. Commun. 4, 2705.
Bolger, A.M., Lohse, M., Usadel, B., 2014. Trimmomatic: a flexible trimmer for Illumina sequence data. Bioinformatics 30 (15), 2114–2120.
Breitburg, D., Levin, L.A., Oschlies, A., Gregoire, M., Chavez, F.P., Conley, D.J., Garcon, V., Gilbert, D., Gutierrez, D., Isensee, K., et al., 2018. Declining oxygen in the global ocean and coastal waters. Science 359 (6371), eaam7240.
Buchfink, B., Xie, C., Huson, D.H., 2015. Fast and sensitive protein alignment using DIAMOND. Nat. Methods 12 (1), 59–60.
Carvalho, I.T., Santos, L., 2016. Antibiotics in the aquatic environments: a review of the European scenario. Environ. Int. 94, 736–757.
Chen, C.-T.A., Guo, X., 2020. Changing Asia-Pacific Marginal Seas. Springer Singapore, Singapore.
Chen, C.-C., Gong, G.-C., Shiah, F.-K., 2007. Hypoxia in the East China Sea: one of the largest coastal low-oxygen areas in the world. Mar. Environ. Res. 64 (4), 399–408.
Chen, W., Ren, K., Isabwe, A., Chen, H., Liu, M., Yang, J., 2019. Stochastic processes shape microeukaryotic community assembly in a subtropical river across wet and dry seasons. Microbiome 7 (1), 138.
Dang, H., Lovell, C.R., 2016. Microbial surface colonization and biofilm development in marine environments. Microbiol. Mol. Biol. Rev. 80 (1), 91–138.
Fu, L., Niu, B., Zhu, Z., Wu, S., Li, W., 2012. CD-HIT: accelerated for clustering the next-generation sequencing data. Bioinformatics 28 (23), 3150–3152.
Grossart, H.-P., 2010. Ecological consequences of bacterioplankton lifestyles: changes in concepts are needed. Environ. Microbiol. Rep. 2 (6), 706–714.
Guo, Y., Liu, M., Liu, L., Liu, X., Chen, H., Yang, J., 2018. The antibiotic resistome of free-living and particle-attached bacteria under a reservoir cyanobacterial bloom. Environ. Int. 117, 107–115.
Guo, J., Yuan, H., Song, J., Li, X., Duan, L., 2020. Hypoxia, acidification and nutrient accumulation in the Yellow Sea Cold Water of the South Yellow Sea. Sci. Total Environ. 745, 141050.
Harrabi, M., Alexandrino, D.A.M., Aloulou, F., Elleuch, B., Liu, B., Jia, Z., Almeida, C.M. R., Mucha, A.P., Carvalho, M.F., 2019. Biodegradation of oxytetracycline and enrofloxacin by autochthonous microbial communities from estuarine sediments. Sci. Total Environ. 648, 962–972.
Hawley, A.K., Brewer, H.M., Norbeck, A.D., Pasa-Tolic, L., Hallam, S.J., 2014. Metaproteomics reveals differential modes of metabolic coupling among ubiquitous oxygen minimum zone microbes. Proc. Natl. Acad. Sci. U. S. A. 111 (31), 11395–11400.
Hou, W., Yu, J., Shi, H., Xu, J., Chen, S.S., Shaban, S.S., Kim, Y., Bai, J., 2025. As a reservoir of antibiotic resistance genes and pathogens, the hydrodynamic characteristics drive their distribution patterns in Lake Victoria. Environ. Pollut. 370, 125903.
Huang, H., Lin, L., Bu, F., Su, Y., Zheng, X., Chen, Y., 2022. Reductive stress boosts the horizontal transfer of plasmid-borne antibiotic resistance genes: the neglected side of the intracellular redox spectrum. Environ. Sci. Technol. 56 (22), 15594–15606.
Hyatt, D., Chen, G.-L., Locascio, P.F., Land, M.L., Larimer, F.W., Hauser, L.J., 2010. Prodigal: prokaryotic gene recognition and translation initiation site identification. BMC Bioinformatics 11 (8), 119.
Jia, B., Raphenya, A.R., Alcock, B., Waglechner, N., Guo, P., Tsang, K.K., Lago, B.A., Dave, B.M., Pereira, S., Sharma, A.N., et al., 2017. CARD 2017: expansion and model-centric curation of the comprehensive antibiotic resistance database. Nucleic Acids Res. 45 (D1), D566–d573.
Jong, M.-C., Harwood, C.R., Blackburn, A., Snape, J.R., Graham, D.W., 2020. Impact of redox conditions on antibiotic resistance conjugative gene transfer frequency and plasmid fate in wastewater ecosystems. Environ. Sci. Technol. 54 (23), 14984–14993.
Karstensen, J., Stramma, L., Visbeck, M., 2008. Oxygen minimum zones in the eastern tropical Atlantic and Pacific oceans. Prog. Oceanogr. 77 (4), 331–350.
Keeling, R.F., Kortzinger, A., Gruber, N., 2010. Ocean deoxygenation in a warming world. Ann. Rev. Mar. Sci. 2, 199–229.
Kojima, S., Koyama, S., Ka, M., Saito, Y., Parrish, E.H., Endo, M., Takata, S., Mizukoshi, M., Hikino, K., Takeda, A., et al., 2023. Mobile element variation contributes to population-specific genome diversification, gene regulation and disease risk. Nat. Genet. 55 (6), 939–951.
Larsson, D.G.J., Flach, C.-F., 2022. Antibiotic resistance in the environment. Nat. Rev. Microbiol. 20 (5), 257–269.
Li, H., Handsaker, B., Wysoker, A., Fennell, T., Ruan, J., Homer, N., Marth, G., Abecasis, G., Durbin, R., Subgroup GPDP, 2009. The sequence alignment/map format and SAMtools. Bioinformatics 25 (16), 2078–2079.
Li, D., Luo, R., Liu, C.-M., Leung, C.-M., Ting, H.-F., Sadakane, K., Yamashita, H., Lam, T.-W., 2016. MEGAHIT v1.0: a fast and scalable metagenome assembler driven by advanced methodologies and community practices. Methods 102, 3–11.
Li, F., Mai, Z., Qiu, C., Long, L., Hu, A., Huang, S., 2023. Dissemination of antibiotic resistance genes from the Pearl River estuary to adjacent coastal areas. Mar. Environ. Res. 188, 105978.
Liu, Y., Ma, Y., Ma, Z., Han, X., Qi, H., Andersen Jens, B., Xu, H., Tolker-Nielsen, T., Qiao, M., 2021. Redox protein OsaR (PA0056) regulates dsbM and the oxidative stress response in Pseudomonas aeruginosa. Antimicrob. Agents Chemother. 65 (3) e01771–01720.
Liu, S., Chen, Q., Liu, L., Dong, C., Qiu, X., Tang, K., 2024. Organic matter composition fluctuations disrupt free-living bacterial communities more than particle-associated bacterial communities in coastal waters. Sci. Total Environ. 949, 174845.
Luo, L., Li, S., Wang, D., 2009. Hypoxia in the Pearl River estuary, the South China Sea, in July 1999. Aquat. Ecosyst. Health Manag. 12 (4), 418–428.
Lyautey, E., Bonnineau, C., Billard, P., Loizeau, J.-L., Naffrechoux, E., Tlili, A., Topp, E., Ferrari, B.J.D., Pesce, S., 2021. Diversity, functions and antibiotic resistance of sediment microbial communities from Lake Geneva are driven by the spatial distribution of anthropogenic contamination. Front. Microbiol. 12, 738629.
Meinhard, S., Hans-Peter, G., Bernd, S., Helle, P., 2002. Microbial ecology of organic aggregates in aquatic ecosystems. Aquat. Microb. Ecol. 28 (2), 175–211.
Shinohara, R., Matsuzaki, S.-I.S., Watanabe, M., Nakagawa, M., Yoshida, H., Kohzu, A., 2023. Heat waves can cause hypoxia in shallow lakes. Geophys. Res. Lett. 50 (8), e2023GL102967.
Siguier, P., Perochon, J., Lestrade, L., Mahillon, J., Chandler, M., 2006. ISfinder: the reference centre for bacterial insertion sequences. Nucleic Acids Res. 34(Database issue):D32-36.
Sloan, W.T., Lunn, M., Woodcock, S., Head, I.M., Nee, S., Curtis, T.P., 2006. Quantifying the roles of immigration and chance in shaping prokaryote community structure. Environ. Microbiol. 8 (4), 732–740.
Stramma, L., Johnson, G.C., Sprintall, J., Mohrholz, V., 2008. Expanding oxygen-minimum zones in the tropical oceans. Science 320 (5876), 655–658.

Tan, H.-J., Cai, R.-S., Bai, D.-P., Hilmi, K., Tonbol, K., 2023. Causes of 2022 summer marine heatwave in the East China seas. Adv. Clim. Chang. Res. 14 (5), 633–641.
Team RC, 2022. R: A Language and Environment for Statistical Computing. R Foundation for Statistical Computing, Vienna, Austria.
Vaquer-Sunyer, R., Duarte, C.M., 2008. Thresholds of hypoxia for marine biodiversity. Proc. Natl. Acad. Sci. U. S. A. 105 (40), 15452–15457.
Wakelin Steven, A., Colloff Matt, J., Kookana Rai, S., 2008. Effect of wastewater treatment plant effluent on microbial function and community structure in the sediment of a freshwater stream with variable seasonal flow. Appl. Environ. Microbiol. 74 (9), 2659–2668.
Wen, L., Dai, J., Song, J., Ma, J., Li, X., Yuan, H., Duan, L., Wang, Q., 2024. Antibiotic resistance genes (ARGs) and their eco-environmental response in the Bohai Sea sediments. Mar. Pollut. Bull. 208, 116979.
Wen, L., Dai, J., Song, J., Ma, J., Li, X., Yuan, H., Duan, L., Wang, Q., 2025. Antibiotic resistance genes (ARGs) in microorganisms and their indications for the nitrogen/sulfur cycle in the East China Sea sediments. J. Hazard. Mater. 488, 137280.
Xu, N., Qiu, D., Zhang, Z., Wang, Y., Chen, B., Zhang, Q., Wang, T., Hong, W., Zhou, N.-Y., Penuelas, J., et al., 2023. A global atlas of marine antibiotic resistance genes and their expression. Water Res. 244, 120488.
Yan, C., Yang, Y., Zhou, J., Liu, M., Nie, M., Shi, H., Gu, L., 2013. Antibiotics in the surface water of the Yangtze estuary: occurrence, distribution and risk assessment. Environ. Pollut. 175, 22–29.
Yezli, S., Li, H., 2012. Antibiotic resistance amongst healthcare-associated pathogens in China. Int. J. Antimicrob. Agents 40 (5), 389–397.
Zhang, Q.-Q., Ying, G.-G., Pan, C.-G., Liu, Y.-S., Zhao, J.-L., 2015. Comprehensive evaluation of antibiotics emission and fate in the river basins of China: source analysis, multimedia modeling, and linkage to bacterial resistance. Environ. Sci. Technol. 49 (11), 6772–6782.
Zhang, Z., Zhang, Q., Wang, T., Xu, N., Lu, T., Hong, W., Penuelas, J., Gillings, M., Wang, M., Gao, W., et al., 2022. Assessment of global health risk of antibiotic resistance genes. Nat. Commun. 13 (1), 1553.
Zhao, D., Gao, P., Xu, L., Qu, L., Han, Y., Zheng, L., Gong, X., 2021. Disproportionate responses between free-living and particle-attached bacteria during the transition to oxygen-deficient zones in the Bohai seawater. Sci. Total Environ. 791, 148097.
Zheng, D., Yin, G., Liu, M., Chen, C., Jiang, Y., Hou, L., Zheng, Y., 2021. A systematic review of antibiotics and antibiotic resistance genes in estuarine and coastal environments. Sci. Total Environ. 777, 146009.
Zhu, Y.-G., Zhao, Y., Li, B., Huang, C.-L., Zhang, S.-Y., Yu, S., Chen, Y.-S., Zhang, T., Gillings, M.R., Su, J.-Q., 2017. Continental-scale pollution of estuaries with antibiotic resistance genes. Nat. Microbiol. 2 (4), 16270.